Development 130, 3917-3928

doi:10.1242/dev.00600

nil per os encodes a conserved RNA recognition motif protein required for morphogenesis and cytodifferentiation of digestive organs in zebrafish

Alan N. Mayer[1,2,*] and Mark C. Fishman[1,†]

[1]Cardiovascular Research Center, Department of Medicine, Massachusetts General Hospital and Harvard Medical School, Charlestown, MA 02129, USA
[2]Pediatric Gastroenterology Unit, Deptartment of Pediatrics, Massachusetts General Hospital and Harvard Medical School, Charlestown, MA 02129, USA
[†]Present address: Novartis Institutes for Biomedical Research, 400 Tech Square, 7th floor, Cambridge, MA 02139, USA
*Author for correspondence (e-mail: mayer@cvrc.mgh.harvard.edu)

Accepted 14 May 2003

SUMMARY

Digestive organ development occurs through a sequence of morphologically distinct stages, from overtly featureless endoderm, through organ primordia to, ultimately, adult form. The developmental controls that govern progression from one stage to the next are not well understood. To identify genes required for the formation of vertebrate digestive organs we performed a genetic screen in zebrafish. We isolated the *nil per os* (*npo*) mutation, which arrests morphogenesis and cytodifferentiation of the gut and exocrine pancreas in a primodial state. We identified the *npo* gene by positional cloning. It encodes a conserved protein, with multiple RNA recognition motifs, that is related to the yeast protein Mrd1p. During development *npo* is expressed in a dynamic fashion, functioning cell autonomously to promote organ cytodifferentiation. Antisense-mediated knockdown of *npo* results in organ hypoplasia, and overexpression of *npo* causes an overgrowth of gastrointestinal organs. Thus, *npo* is a gene essential for a key step in the gut morphogenetic sequence.

Key words: Zebrafish, Genetics, Intestine, Digestive system, Embryology, RNA-binding proteins

INTRODUCTION

All vertebrates undergo similar morphogenetic steps in forming the digestive organs (Grapin-Botton and Melton, 2000). After specification of the endoderm, the primitive gut tube represents the first morphologically recognizable precursor of the alimentary tract. The undifferentiated endoderm that lines the gut tube ultimately gives rise to the parenchyma of the digestive organs and other derivatives, such as the lungs and thyroid. How overtly featureless tissue becomes specified to particular organ fates – adopting a genetically determined size, shape and cytoarchitecture – is not known. The genetic programs that guide the formation of organs during embryonic life may also be utilized later for repair and homeostasis, and, in some cases, may become unregulated and promote carcinogenesis. Therefore, identifying the crucial genetic components that guide organogenesis, and ultimately assembling these elements into coherent pathways, has relevance to a broad array of medical problems.

Organogenesis is conventionally framed by morphogenetic events, and as molecular insight accrues, the morphogenetic framework is annotated with details of expression patterns and gene activities. For the intestine, morphogenesis of the adult form begins with aggregations of mesenchyme beneath the epithelium to create the beginnings of intestinal villi. These changes are accompanied by epithelial cytodifferentiation, marked by the acquisition of apical-basal cell polarity and the initiation of lineage-specific gene expression programs (Montgomery et al., 1999; Roberts, 1999). Individual aspects of the anlage-to-organ transition have been linked to single genes. For example, genetic control has been demonstrated for villus number (Karlsson et al., 2000) or form (Kaestner et al., 1997), goblet cell differentiation (Katz et al., 2002) or secretory cell specification (Yang et al., 2001). Yet to our knowledge, there are no reports of mutations that arrest development after primitive gut tube morphogenesis but before the initiation of villi formation. Thus it is not known whether global regulation of this step exists, or whether such regulation might be genetically dissectible.

A similar question can be formulated for the pancreas and liver. These anlage bud from the primitive gut tube, expressing both endoderm-specific and, progressively, organ-specific genes. The pancreatic anlage expresses Pdx1, then matures through cell fate decisions that lead to islet cells and exocrine cells (Edlund, 1999). The exocrine pancreas then grows and differentiates under the influence of factors produced by the adjacent mesenchyme (Wessells and Cohen, 1967). The logic of pancreas development has become clearer in recent years, as genetic and embryologic studies have related specific signaling pathways to discrete steps of the developmental sequence (Kim and Hebrok, 2001). The liver is distinguished

by expression of organ-specific genes even before the anlage becomes morphologically detectable, but its subsequent outgrowth is also controlled by interactions with surrounding tissues (Zaret, 2000).

Classic genetic studies of development have proven their utility in creating a molecular underpinning for the metazoan body plan, but the model organisms exploited to create that framework, *Drosophila* and *C. elegans*, lack many of the organs found in vertebrates. Taking our cue from this powerful approach, we sought to discover whether there are genes that, when mutated, would freeze the developing vertebrate digestive tract in an undifferentiated state. We therefore conducted a genetic screen in zebrafish. Here, we describe the positional cloning and characterization of *npo (nil per os*, Latin for 'nothing by mouth'). We show that *npo* encodes a conserved RNA recognition motif protein that is dynamically expressed in the embryonic digestive tract, the requirement for which defines a novel control point during organogenesis.

MATERIALS AND METHODS

Zebrafish strains and studies

Care and breeding of zebrafish *Danio rerio* was performed as described (Westerfield, 1995). Developmental staging was carried out using standard morphological features (Kimmel et al., 1995) of fish raised at 28.5°C.

Mutagenesis and screening

Males of the TL line were treated with ENU as described previously (Haffter et al., 1996), bred with wild-type females for at least two generations, then in-crossed to drive recessive mutations to homozygosity. Live inbred progeny were examined at 4 days postfertilization (dpf) using a Wild M10 dissecting microscope.

Histologic methods

Fixation of embryos for histology, embedding in JB-4 (Polysciences) and plastic sectioning was performed as described previously (Pack et al., 1996). Embryos for electron microscopy were fixed in 2% glutaraldehyde in 0.1 M sodium cacodylate buffer (pH 7.4) overnight at 4°C. Embryos were rinsed in buffer, post-fixed in 1% osmium tetroxide in cacodylate buffer for 1 hour at room temperature, rinsed again in buffer, then in distilled water and stained, en bloc, in an aqueous solution of 2% uranyl acetate for 1 hour at room temperature. They were rinsed in distilled water and dehydrated through a graded series of ethanol to 100%. They were further dehydrated in 100% propylene oxide and then infiltrated with Epon resin (Electron Microscopy Sciences, Fort Washington, PA) in a 1:1 solution of Epon:propylene oxide. The following day they were placed in fresh Epon for several hours and then embedded in Epon overnight at 60°C. Thin sections were cut on a Reichert Ultracut E ultramicrotome, collected on formvar-coated slot grids, stained with uranyl acetate and lead citrate, and examined using a Philips CM 10 transmission electron microscope at 80 kV.

Cartilage staining

Jaw and brachial arch structures were visualized using Alcian Blue as described (Schilling et al., 1996).

Immunofluorescence

Embryos for Zo1 and ATPase antibody staining were fixed in Dent's solution [80% methanol, 20% DMSO (v/v)] overnight at 4°C, and then stored in methanol at –20°C. Whole embryos were stained as described previously (Westerfield, 1995) and embedded in JB-4 for sectioning. Slides were mounted with Gel-mount (Fisher) and photographed using a Zeiss Axiophot. For Npo immunostaining of embryos, paraffin sections were permeabilized by digesting with 10 mg/ml proteinase K for 20 minutes, then post-fixed with 4% paraformaldehyde for 20 minutes at room temperature. After washing several times with phosphate buffered saline containing 0.1% Tween-20 (PBT), the tissue was blocked with PBT containing 1% bovine serum albumin (BSA) and 10% sheep serum (Sigma). Blocking solution was replaced with anti-Npo at a concentration of 1 μg/ml in blocking solution. The sections were incubated for 2 hours at room temperature, then washed six times in PBT-1% BSA before incubation with secondary antibody (Cy-3-conjugated sheep anti-rabbit; Rockland). Controls containing no primary antibody were included with all experiments. Antibodies were obtained as follows: mouse monoclonal anti-zo1 (S. Tsukita); mouse monoclonal anti-ATPase-α5f subunit (Developmental Studies Hybridoma Bank). Polyclonal antipeptide antibodies to the Zebrafish Npo protein were generated by immunizing rabbits with a peptide of amino acids 122-137 (CLNVLGDLEKDESFQEF) (antibody 4151), followed by affinity purification (QCB/Biosource International). Conjugated secondary antibodies were from Sigma or Rockland Immunochemicals.

Positional cloning

The *npo*$^{fW07\text{-}g}$ (TL background) mutation was mapped by out-crossing into the polymorphic wild-type strain WIK, followed by inbreeding of heterozygous progeny. We scanned the genome for linkage by bulked-segregant analysis (Shimoda et al., 1999), which placed the *npo* mutation on linkage group 6. Fine mapping identified marker z8532 to be 0.03 cM (1/2971) from the *npo* locus. A chromosome walk was performed from z8532, and the genetic interval covered with 2 BACs, 37b12 and 90p3 from the BAC library distributed by Incyte Genomics (Amemiya et al., 1999). These were subjected to shotgun sequencing, and the assembled sequence encoded a single contig 129 kb in length, which contained four open reading frames predicted by both homology to GenBank sequences (blastx) and by the exon prediction program GENESCAN from the MIT website (http://genes.mit.edu/GENSCAN.html). Internal genetic markers were generated from simple-sequence repeats found within the contig and used to narrow the genetic interval further. The two remaining candidates were analyzed by complete sequencing of cDNAs isolated by RT-PCR from mutant and wild-type embryos. The candidate *epha2* cDNA did not contain any detectable mutations, whereas the RRM-encoding cDNA was found to have a nonsense mutation at codon 221 of the 926 codon reading frame. This result was substantiated by sequencing PCR products from genomic DNA derived from 12 mutants, 12 phenotypically wild-type siblings and 12 wild types. The GenBank Accession Number for zebrafish *npo* is AY299514.

In vitro transcription/translation

Total RNA was isolated from ~50 *npo*-mutant and 50 wild-type embryos at 4 dpf using Trizol reagent (Life Technologies) according to manufacturer's instructions. We used a combination of dT and randomly primed cDNA as a template for two rounds of nested PCR to amplify the full-length cDNAs. The DNA polymerase used was Pfu-Turbo (Stratagene), and Taq polymerase was used to add a 3′ adenine for cloning into pCRII (Topo-TA kit, Invitrogen). We isolated 12 independent clones and sequenced these completely. The in vitro coupled transcription/translation was performed using the T7 TNT system (Promega). [^{35}S]-methionine-labeled protein was electrophoresed on a 10% SDS-polyacrylamide gel, followed by autoradiography.

RNA binding assays

Npo protein sythesized as above was assayed for RNA homopolymer binding activity essentially as described previously (Swanson and Dreyfuss, 1988). Briefly, homopolymeric RNA bound to solid agarose support was purchased from commercial sources (poly C and poly U from Sigma; poly G and poly A from Pharmacia). The beads were

suspended and washed extensively in binding buffer [10 mM Tris HCl (pH 7.3), 50 mM NaCl, 2.5 mM $MgCl_2$, 0.1% Tween 20]. In vitro translation products of Npo wild-type, mutant and luciferase control (20 μl, about 100,000 cpm of acid insoluble radioactivity) were added to ~100 μg of beads in 1 ml of binding buffer, and incubated with rocking at room temperature for 10 minutes. The beads were washed six times with binding buffer, then boiled in 25 ml SDS-PAGE sample buffer (Chantry and Glynn, 1986) for 5 minutes and loaded onto a 10% SDS-polyacrylamide gel. After electrophoresis and autoradiography the resulting bands were quantitated by using the program NIH Image 1.62. Percent bound was calculated from the ratio of bound to input radioactivity migrating at the expected molecular weights. Three separate measurements were performed from which the average bound fraction was calculated.

Embryo microinjections

We microinjected 1-cell-stage embryos essentially as described (Westerfield, 1995). The embryos were first dechorionated in pronase and maintained in 0.3×Danieu's medium. The indicated BACs were prepared using Qiagen columns, as instructed by the manufacturer followed by an additional phenol/chloroform extraction and ethanol precipitation. BAC DNA was diluted into Danieu's medium/0.1% Phenol Red (as a tracer) to a final concentration of 100 ng/μl. BAC linearized with *Not*I gave similar results to circular DNA. We monitored cleavage of BAC 37b12 by *Sna*BI by pulsed-field gel electrophoresis and by PCR across the restriction site.

Morpholino antisense oligonucleotides were designed corresponding to the start site and splice junctions of the zebrafish genomic *npo* sequence. The sequences were as follows:

–15/+9, CCTTGACATTTTTCTGAGCCAAGT;
+25/int1, ATGAATACTTACCCCATTCGGGAG;
int1/+37, TCCTTCATCTGGAGACACAACATG; and
+909/int, CATTTTATTACAGATTGAGCCAAC.

Concentrations ranged from 0.1 to 0.5 mM, with 0.5 mM giving the most profound effect. Control injections included the sense strand and an oligonucleotide of unrelated sequence, all of which led to no intestinal defects by criteria of histology and *ifabp* expression. Above 0.5 mM we noted a non-specific toxicity based on early abnormalities in control-injected embryos (i.e. sense morpholinos).

In situ hybridization

We carried out probe synthesis and whole-mount RNA in situ hybridization as described (Jowett, 1999). The digoxigenin-labeled RNA probes were generated from the following templates: *ifabp* was generated by RT-PCR from adult zebrafish intestinal mRNA, using primers designed from the published sequence (Andre et al., 2000); the *insulin* probe was generated by RT-PCR of 4 dpf embryonic RNA, using primers designed from published sequence (Milewski et al., 1998); and zebrafish *npo* probes, corresponding to the full-length coding sequence, were generated by *Not*I digestion of pCRII (Invitrogen) containing the *npo* cDNA, followed by in vitro transcription with SP6 RNA polymerase for the antisense probe, and *Spe*I and T7 polymerase for the sense control. *sonic hedgehog (shh), patched1* and *patched2* probes were generously provided by P. Ingham. *foxa2* was described previously (Chen et al., 2001).

Embryos were genotyped subsequent to in situ hybridization for purposes of scoring rescue, or for determining genotype of embryos before 96 hours postfertilization (hpf), when the mutants and wild types can be clearly distinguished. This was done by sectioning a small portion of the tail, placing it into methanol, evaporating the methanol, then digesting the tail in 5 μl of lysis buffer at 50°C overnight to release the DNA. We performed genotyping using either z8532 or, in the case of the injection/rescue, sequence from the SP6 end of BAC 90p3.

Mosaic analysis

Embryos were dechorionated using pronase, and donors were injected with rhodamine-dextran biotin (lysine fixable) from Molecular Probes. From ~4-6 hpf (mid blastula to early epiboly), 5-10 cells were removed from the blastula margin of donors and inserted into the blastula margin of recipients. The embryos were then cultured in the presence of 1:100 penicillin-streptomycin and allowed to develop to 4 dpf. Survival was about 50%. Live recipient embryos were then screened for the presence of red fluorescence in the vicinity of the intestine. Ultimately, less than 10% of the embryos contained label associated with the intestine. In the mutant recipients (in which gut is hard to discern), many of the initial positives were later found to have only pronephric duct staining by histologic analysis. The embryos were then fixed and processed for in situ hybridization to detect *ifabp* expression. To enhance detection of the lineage tracer, the embryos were incubated with Cy-3 streptavidin before embedding and sectioning.

RESULTS

npo mutant isolation

In zebrafish, the key events of organogenesis in the digestive tract are spread over a 3 day period, from about 24 to 84 hours postfertilization (hpf) (Pack et al., 1996). We screened a pool of ENU-mutagenized zebrafish for recessive mutations that interfere with differentiation and growth of the digestive organs, examining live embryos by dissecting microscopy after 96 hpf, a time when the differentiated digestive organs (gut, pancreas, liver) are visible. We identified a mutant allele ($npo^{fw07\text{-}g}$) in which the gut, liver and pancreas could not be detected using a dissecting microscope, yet other organs and structures appeared relatively normal (Fig. 1A,B). The mutation is recessive lethal and 100% penetrant in all backgrounds tested (WIK, TL, Tubingen). Because the mutant larvae do not eat we named the locus *nil per os*. The mutant also has an underdeveloped jaw and branchial arch structures (Fig. 1C,D). Although live mutants appear normal until about 84 hpf, histological sectioning of mutant embryos identified by genotyping reveals developmental defects are first noticeable at about 60-72 hpf. It is at this stage that the gut begins a phase of rapid growth and cytodifferentiation. At 96 hpf, mutant embryos exhibit overall digestive organ hypoplasia, and the absence of differentiated intestinal and exocrine pancreatic epithelium (Fig. 1G,H). Unaffected structures and organs include the notocord, somites, heart, kidney and nervous system.

npo is required for the endoderm-intestine transition

To determine the developmental step at which the *npo* is essential, we assessed mutant embryos for achievement of various developmental milestones. By using whole-mount in situ hybridization, we monitored expression of the *foxa3* and *sonic hedgehog* (*shh*) genes at various time points in *npo*-mutant and wild-type embryos, which allowed us to follow the morphogenesis of endoderm-derived structures through organogenesis (Chen et al., 2001; Odenthal and Nusslein-Volhard, 1998). As shown in Fig. 2A-D, the expression patterns of *foxa3* and *shh* in wild-type and mutant embryos are not discernibly different before 48 hpf. *shh* expressed in the foregut is excluded at the expected site of pancreatic budding, and *foxa3* staining shows the liver and pancreas primordia budding at the same location in wild-type and mutant embryos. We also evaluated the expression of the mesenchymal targets of *shh*,

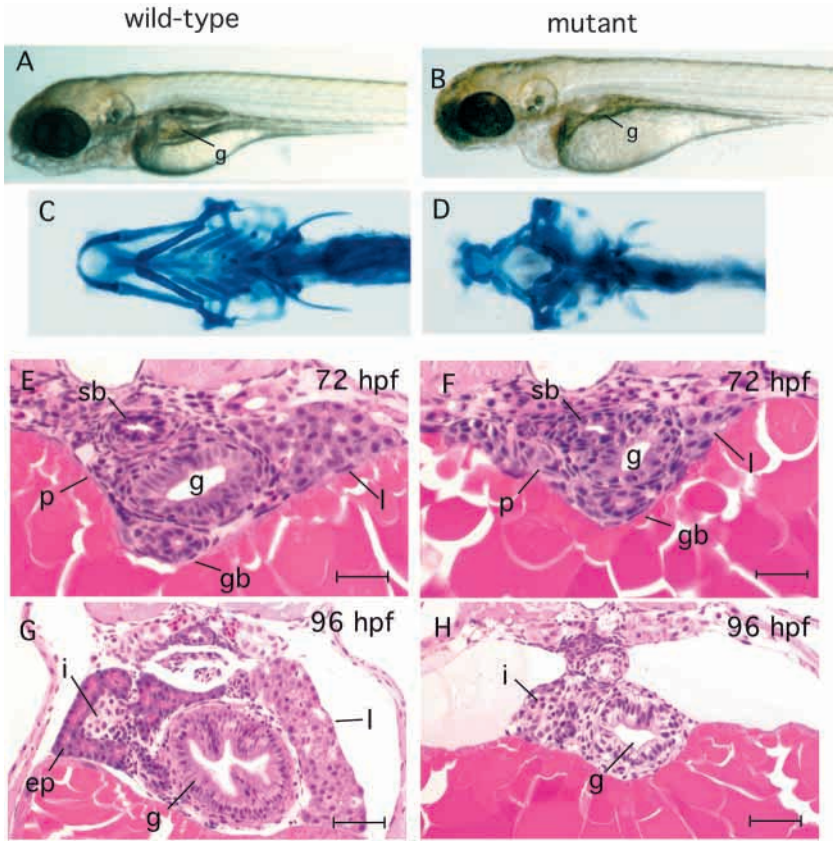

Fig. 1. *npo*-mutant phenotype. (A,B) Live larvae at 4.5 dpf, showing that the jaw, branchial arches and gut tube are markedly underdeveloped at 96 hpf, but that dorsal structures (somites, notocord) appear unaffected by the mutation. (C,D) Alcian Blue staining of wild-type and mutant larvae at 4.5 dpf demonstrates failure of branchial arch growth beyond the initial primordium. (E-G) Cross sections of embryos stained with Hematoxylin and Eosin at the level of the pancreatic islet. (E,F) 72 hpf embryos (genotyped prior to embedding) showing the first morphologically detectable differences between mutant and wild type, with hypoplastic gut and liver in the mutant. (G,H) 96 hpf embryos show a stark contrast between wild type and mutant. The mutant gut tube is substantially smaller and the epithelial architecture is less organized, with no villi formation. The exocrine pancreas is not recognizable in the mutant, yet the islet appears relatively normal. The liver is not seen because it is much smaller in the AP dimension and does not extend to this level. g, gut; p, pancreas; l, liver; i, pancreatic islet; ep, exocrine pancreas; gb, gall bladder; sb, swim bladder. Scale bars: E,F, 20 μm; G,H, 30 μm.

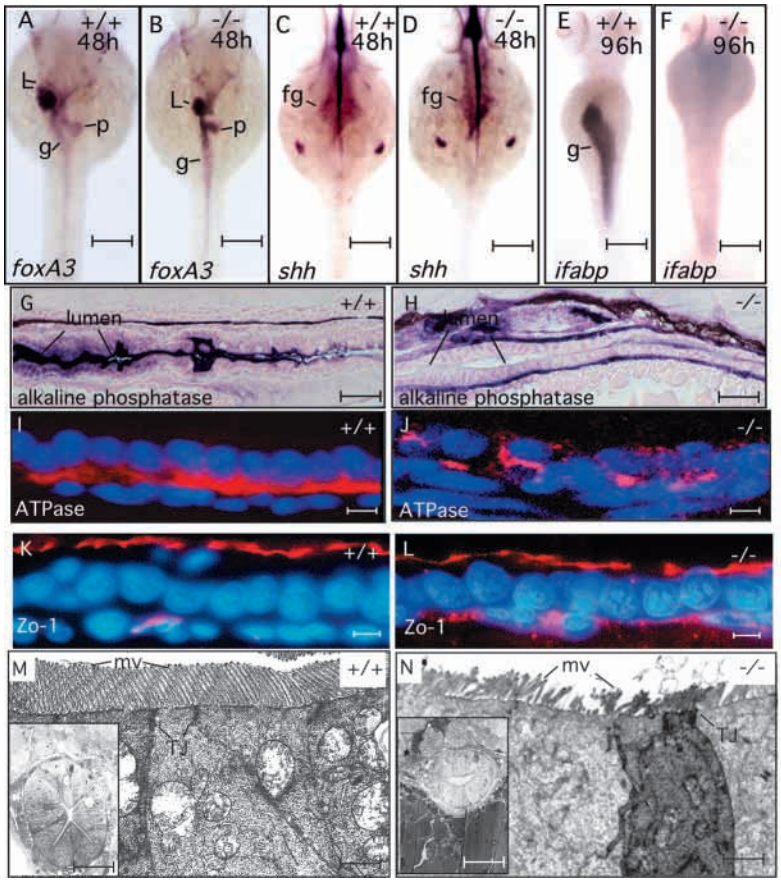

Fig. 2. *npo* is required for endoderm-intestine transition. (A,B) *foxa3* expression pattern at 48 hpf showing formation of liver, gut and pancreatic anlage in both wild-type and *npo* mutant embryos. (C,D) *shh* expression at 48 hpf reveals normal foregut patterning, with label exclusion at the prepancreatic endoderm. (E,F) *ifabp* expression detected in the wild-type intestine but not in the mutant. (G,H) Histochemical staining for alkaline phosphatase. Robust staining of apical aspect of epithelium in the wild type, but staining of mutant epithelial cells appears basal, suggesting mislocalization. (I,J), Na/K ATPase immunofluorescence demonstrates basolateral localization of fluorescence in wild type, but no clear localization in the mutant. (K,L) Zo1 immunofluorescence demonstrates formation of zona occludens in both wild-type and mutant embryos. (M,N) Transmission electron micrograph of intestine. Junctional complexes are present in both mutant and wild-type epithelia. Microvilli in the wild type are smooth and uniform, but in the mutant they are fewer and pleiomorphic. +/+, wild type; –/–, mutant; g, gut; L, liver; p, pancreas; mv, microvilli; TJ, tight junction. Scale bars: A-F, 150 μm; G,H, 20 μm; I-L, 10 μm; M,N, 1 μm; insets, 30 μm.

ptc1 and *ptc2* (Lewis et al., 1999), and *bmp4* (Chen et al., 1997), as well as endodermal markers *foxa2* (*axial*) (Odenthal and Nusslein-Volhard, 1998), *tcf4* (Dorsky et al., 1999), *gata5* (Pack et al., 1996) and *pescadillo* (Allende et al., 1996). We noted no differences in expression patterns by in situ hybridization at 48 hpf (data not shown).

At about 48 hpf, gut tube morphogenesis occurs by canalization of the endoderm and formation of tight junctions between the epithelial cells (Horne-Badovinac et al., 2001). Electron microscopy and Zo1 immunofluorescence staining of 96 hpf embryos shows that tight junctions do form between the gut epithelial cells (Fig. 2I,J). Brush border microvilli also are present in the mutant, but they are fewer in number and misshapen (Fig. 2M,N).

After the gut tube forms, the endodermal cells re-organize into a simple columnar epithelium and begin to express organ-specific genes. For the gut, this is the key distinguishing step that marks the transition to mature organ, and it has been previously termed the 'endoderm-intestine transition' (Traber and Wu, 1995). In the zebrafish, this transition occurs between 60 and 72 hpf, when the intestinal epithelial cells begin to express alkaline phosphatase. Histochemical localization to the apical aspect of the epithelial cell reflects establishment of apical-basal polarity (Pack et al., 1996). Alkaline phosphatase staining is absent from the apical aspect of the mutant gut epithelium at 96 hpf, and appears to be basally localized (Fig. 2G,H). Immunofluorescence detection of the Na/K ATPase-α6f subunit, which is normally localized to the basolateral surface of wild-type epithelial cells, reveals no clear localization in the mutant. Expression of the enterocyte-specific gene encoding intestinal fatty acid binding protein (*ifabp*) becomes detectable in the foregut of the wild-type embryo between 72 and 84 hpf, and expression expands caudally (Andre et al., 2000); however, no expression is detected in the mutant intestine by 96 hpf (Fig. 2E,F). Taken together, these data point to a step early in gut cytodifferentiation for which *npo* is essential.

npo is required for liver and exocrine pancreas development

In wild-type and mutant embryos, the pancreatic bud forms from the primitive gut tube at the proper location, as shown in Figs 2, 3. But histological sectioning of the mutant embryos at 96 hpf shows a pancreatic islet surrounded by only a rim of flat cells, rather than distinct acinar cells of the exocrine pancreas (Fig. 1G,H). *trypsin* gene expression and immunoreactive carboxypeptidase are not detected in the mutant, which is consistent with a failure to form the exocrine pancreas (Fig. 3). By contrast, the pancreatic islet does form in the mutant, as seen by histological examination (Fig. 1G,H), and based on presence of insulin expression (Fig. 3E-H).

The liver bud is morphologically detectable at about 40 hpf in both wild type and *npo* mutants, but in the mutant it never grows larger than that of a normal 72 hpf embryo. Bile synthesis and secretion does occur in the mutant based on the appearance of bright yellow material in the intestinal lumen. Staining for carbohydrate with periodic acid-Schiff reagent reveals glycogen in the hepatocytes in both mutant and wild-type embryos (data not shown). Despite these signs of hepatocyte differentiation, the mutant hepatocytes fail to express immunoreactive cytokeratin (Fig. 3). Thus, the *npo* requirement in liver development appears to occur toward the later phases of hepatogenesis.

In summary, the unifying feature of the organ-specific defects we observe in the *npo* mutant is the arrest of development just after the appearance of the endodermal organ primordia, the 'anlage', but prior to growth and specific cellular distinction into mature epithelial cells of the gut, liver and

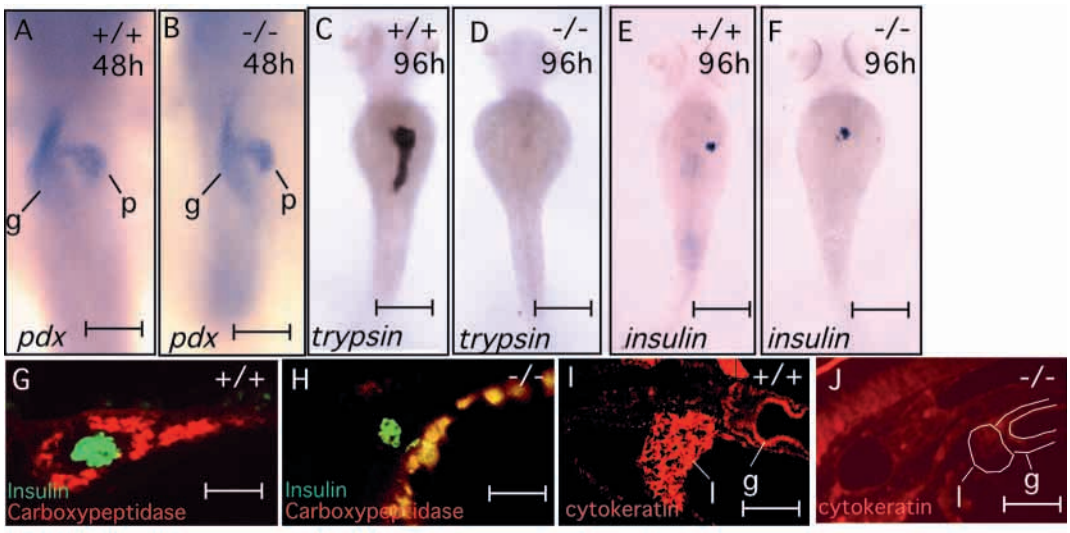

Fig. 3. *npo* mediates exocrine pancreas and liver cytodifferentiation. (A-F) Whole-mount in situ hybridizations show formation of pancreatic primordia in both mutant and wild-type embryos at 48 hpf (A,B), and subsequent failure to form differentiated exocrine pancreas in mutant embryos by 96 hpf (C,D). By contrast, islet formation is independent of *npo*. (G,H), Double immunofluorescence staining for insulin (green) and carboxypeptidase (red) shows selective failure of exocrine pancreas formation in the mutant, with sparing of the pancreatic islet. (I,J) Immunofluorescence detection of cytokeratin (monoclonals AE1/AE3), demonstrating staining of wild-type liver and gut epilthelia, but absent specific staining of mutant epithelia. White outline defines organ boundaries identified by phase contrast. g, gut; p, pancreas; l, liver. Scale bars: A,B, 80 μm; C-E, 150 μm; G-J, 25 μm.

exocrine pancreas. This suggests that *npo* is crucial in traversing a key epithelial maturation step in these endodermal derivatives.

Positional cloning of *npo*

We identified the *npo* gene by positional cloning (Fig. 4). We mapped *npo* to a 0.06 cM genetic interval, within which we identified two genes. One of these encodes Epha2, in which we did not identify any coding mutations, and the overexpression of which by cDNA and BAC injection does not rescue the phenotype. The other gene, *npo*, encodes a hypothetical RNA-recognition motif (RRM) protein. The mutant allele has a T to A mutation, which results in a premature termination codon at position 221 of the predicted 926 amino acid sequence. In vitro coupled transcription/translation of *npo* cDNA obtained from wild-type and mutant embryonic RNA conforms to this size prediction (104 kDa and 25 kDa, respectively), which is consistent with truncation of the protein in the mutant.

We designed several morpholino antisense oligonucleotides to the candidate *npo* gene. All four *npo*-antisense oligonucleotides abrogate the formation of mature intestinal or exocrine pancreatic epithelium. The expression of insulin, which is present in the *npo* mutant, is also present in the morpholino-injected embryos (Fig. 5). Branchial arches, as monitored by Alcian Blue staining, are completely absent in the morpholino-injected embryos (data not shown).

Rescue and overexpression

Injection of cDNA encoding *npo* under the control of a CMV promoter resulted in a high frequency of gastrulation defects, which precluded our using this tactic for rescue of the *npo* phenotype. The BAC containing the candidate *npo* gene (BAC 37b12) rescues the *npo* phenotype when injected into 1- to 4-cell-stage embryos (Fig. 5), and the effect is blocked by co-injection of a *npo*-specific morpholino antisense oligonucleotide. 70 out of 82 genotypically mutant embryos injected with 37b12 were rendered *ifabp* positive, giving a rescue efficiency of 85%. Using *trypsin* as the probe, we obtained a similar result with rescue of 32 out of 47 genotypically mutant embryos (68% efficiency). Rescue of the branchial arch phenotype appears to occur less reliably, with marginally increased but disorganized cartilage detected in the BAC-injected embryos. Control injections included BAC 90p3 (which contains the entire coding and promoter sequence for the adjacent *epha2* gene), and BAC 37b12 treated with the endonuclease *Sna*BI. The latter specifically disrupts the *npo* gene between exons 1 and 2. These controls both failed to show any rescue activity (*ifabp* or *trypsin* expression) in the mutant embryos.

In the course of the rescue experiments, we noted that the expression domain for *ifabp* and *trypsin* in many of the BAC 37b12-injected embryos seemed expanded relative to uninjected wild type and the other controls (Fig. 5). Indeed, in many cases the BAC 37b12-injected embryos contain an exuberant overproduction of differentiated intestinal or exocrine pancreatic epithelium. The individual epithelial cells do not appear abnormal, but the overall size of the gut tube, the number of epithelial infoldings and the size of the exocrine pancreas is dramatically increased. Thus it appears that the increased copy number resulting from BAC injection can overwhelm the normal control of *npo* gene expression, and this leads to increased amounts of mature organ tissue.

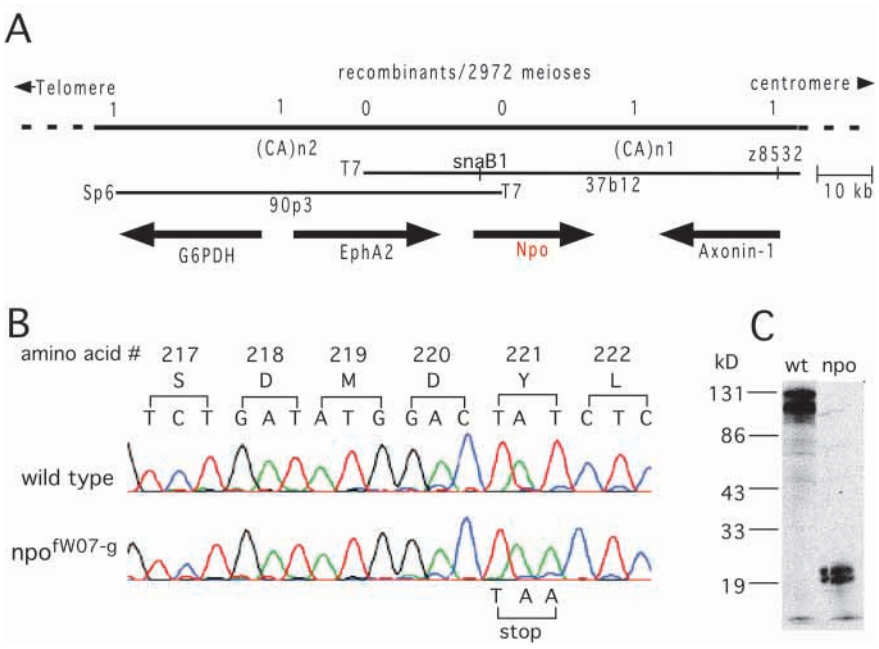

Fig. 4. Positional cloning of *npo*. (A) Integrated genetic/physical map depicting chromosome walk across the *npo* locus, initiated at microsatellite marker z8532. Two overlapping BACs covered the *npo* interval, and these were subjected to complete sequencing, resulting in a 129 kb contig. Within this interval, we identified four genes and new microsatellite markers. These were used to genotype the flanking recombinants and to exclude the two outer genes. Thus only *epha2* and a hypothetical RRM protein encoding gene fine-mapped within the genetic locus. We isolated full-length cDNAs corresponding to both genes from homozygous-*npo* mutant and wild-type embryos, and six independent clones from each were completely sequenced in both directions. No mutations were found in the *epha2* coding sequence, whereas a T to A (encoding a Y to stop) mutation was identified in the RRM-encoding gene, which we designated *npo*. (B) Sequence tracing of one of 12 independent clones derived from PCR of genomic DNA from mutant and wild-type embryos, showing TAT (Y) to TAA (stop) mutation. (C) cDNA from wild-type and mutant embryos subjected to in vitro transcription/translation produces a truncation of mutant Npo, in agreement with the conceptual translation. The doublet most likely arises from an alternate translation start site.

npo encodes a conserved RRM protein

Conceptual translation of the cDNA indicates that Npo is related to a protein conserved through evolution (Fig. 6). In all metazoans, the gene for this protein encodes six consensus RNA recognition motifs (RRMs). In yeast and plants, the orthologous gene encodes five RRMs (without domain 2, which is the least conserved among metazoans). As shown in Fig. 6, domain order and spacing are generally conserved. The highest amino acid homology between species occurs within the RRM domains, ranging from 30% to 75% identity. The biochemical function of the related yeast

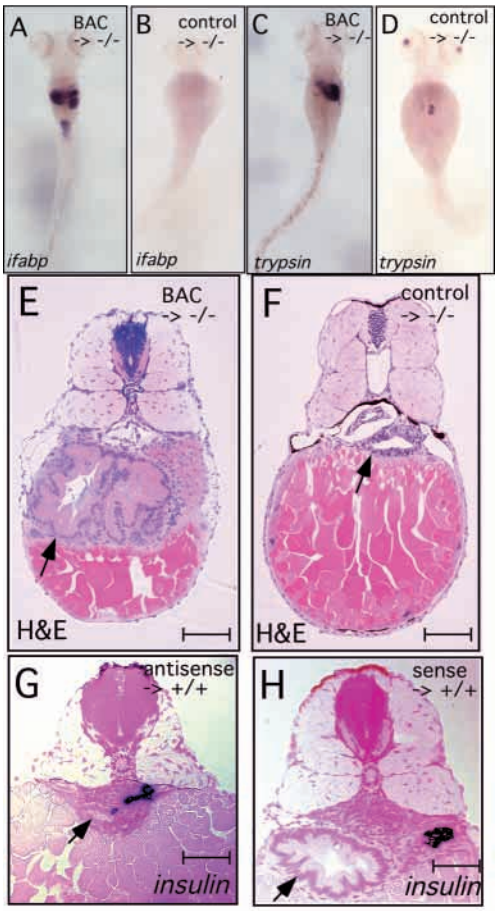

Fig. 5. Rescue and phenocopy of *npo* mutation. (A,C,E) 96 hpf *npo*-mutant embryos that had been injected with *Not*I-digested BAC 37b12 at the 1-cell stage. (B,D,F) Mutants injected with BAC 37b12 pre-cut with restriction endonucleases *Not*I and *Sna*BI, which cuts only between the first and second exon of the *npo* gene. (G,H) Wild-type embryos injected with morpholino oligonucleotides encoding antisense and sense sequences, respectively, from the *npo* transcript. (A,B) Representative embryos stained by whole-mount in situ hybridization for *ifabp* show rescue of this marker by BAC 37b12 injection in the expected mosaic pattern, and undetectable rescue observed using the cleaved BAC. By comparing panel A with Fig. 2E, we note that the BAC-injected mutant embryos have a broader *ifabp* expression pattern than the wild-type embryos. (C,D) Staining for *trypsin* demonstrates mosaic rescue of the *npo* phenotype, also with a broader expression pattern than seen in the wild-type (compare with Fig. 3C). The control-injected embryos shows a few cells stained for *trypsin* expression, which we also note occasionally in control-uninjected embryos. (E,F) Embryos shown in A and B, respectively, were sectioned and stained with Hematoxylin and Eosin. This revealed an over-expanded intestinal and exocrine pancreatic epithelium in the embryos injected with intact BAC 37b12, but no histological effect on the mutant phenotype in the control (arrows). (G,H) Histological sections of embryo injected with *npo*-specific morpholino oligonucleotides, sense or antisense as indicated, stained for *insulin* by whole-mount in situ hybridization, then sectioned and counterstained with nuclear Fast Red. Antisense injection leads to hypoplasia, dysmorphogenesis and abrogation of epithelial cytodifferentiation similar to that seen in the *npo*-homozygous mutant. *insulin* expression is not affected, as seen in the homozygous mutant. Normal digestive organs are seen in the sense control. Note, the effects on the digestive organs due to manipulation of *npo* expression often result in uncoupling of the AP axes of the neural tube from the digestive organs. For this reason, we chose internal landmarks in the digestive tract (i.e. islet or gall bladder) rather than neural tube or somite landmarks. Arrows indicate intestine. Scale bars: A-D, 200 μm; E-H, 20 μm.

protein Mrd1p has recently been reported to mediate processing of pre-ribosomal RNA (Jin et al., 2002).

Although the specific targets of Npo are not known, RRM domains in other proteins confer binding to homopolymeric RNA in vitro (Varani and Nagai, 1998). We found that Npo protein, when translated in vitro, does bind homopolymeric RNA with a marked preference for guanine (G) and uracil (U), as opposed to adenosine and cytosine. The truncated-mutant Npo protein also shows a similar nucleotide binding preference, but its binding affinity for polyribonucleotides is reduced (Fig. 6C).

npo is expressed transiently in the digestive tract epithelium

npo is expressed ubiquitously in the early embryo. At about 24 hpf, expression becomes restricted to the brain and anterior digestive tract (Fig. 7E). Expression then increases in an anterior to posterior wave, first in the branchial arches and liver, then spreading posteriorly, until by 72 hpf it is expressed in a uniform manner throughout the digestive organs (Fig. 7). Between 72 and 84 hpf, *npo* expression declines rapidly, from anterior to posterior, leaving a residual stippled pattern of expression in the intestine. Expression of *npo* in the pancreas is excluded from the islet (Fig. 7C), consistent with a lack of effect on this structure in the mutant.

Histological sectioning reveals *npo* expression in the gut epithelium (Fig. 8A-C). The in situ labeling pattern is heterogeneous, suggesting cell-to-cell variation in steady state levels of *npo* mRNA. Also, the labeling pattern appears punctate, which is suggestive of subcellular localization of the message. The focality of *npo* localization is illustrated by double in situ hybridization to *foxa3* and *npo* (Fig. 8B). The former is expressed in all the gut epithelial cells and the labeling pattern is more diffuse. By contrast, the *npo*-specific signal is seen in a subset of the *foxa3*-positive cells and is highly localized.

To detect Npo protein, we developed polyclonal antibodies directed against synthetic peptides. In embryos, we found staining primarily in the gut epithelium (Fig. 8C). The degree of cell-to-cell variation in antibody staining is not as dramatic as that seen in the in situ hybridizations, but it is still present. Npo appears to be localized to the cytoplasm, mostly towards the apical aspect of the cell. We also noted label within in a few cells in the mesenchyme. Preliminary studies suggest that mesenchymal expression in the adult gut is present as well (data not shown).

npo functions cell autonomously during gastrointestinal development

The data suggesting that *npo* is expressed in both the mesenchyme and in the epithelium raises the question of what cell type requires *npo* function for epithelial cytodifferentiation. To address this we performed mosaic analysis, transplanting wild-type blastomere cells into an *npo*-

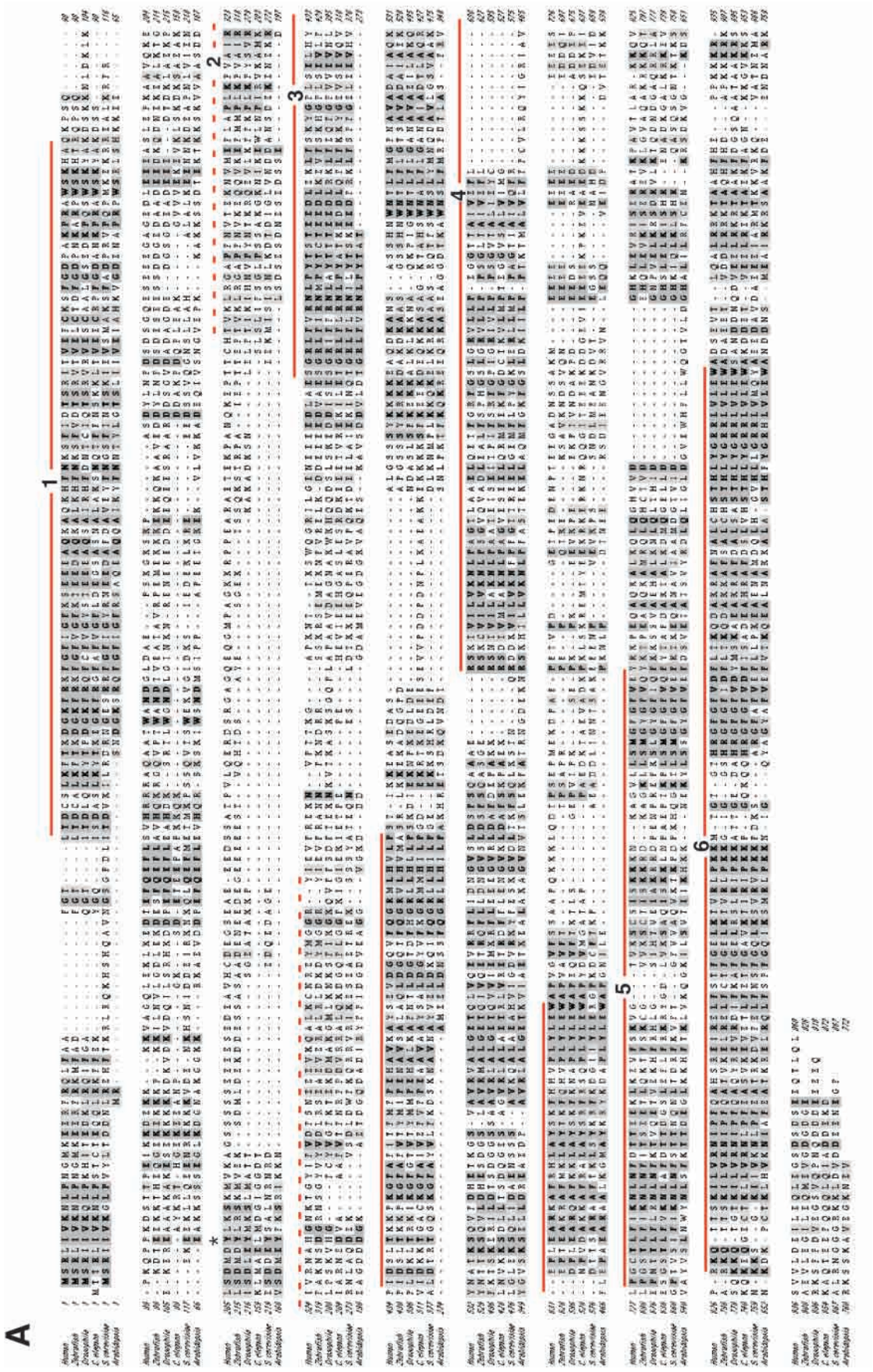
A
1
2
3
4
5
6
*

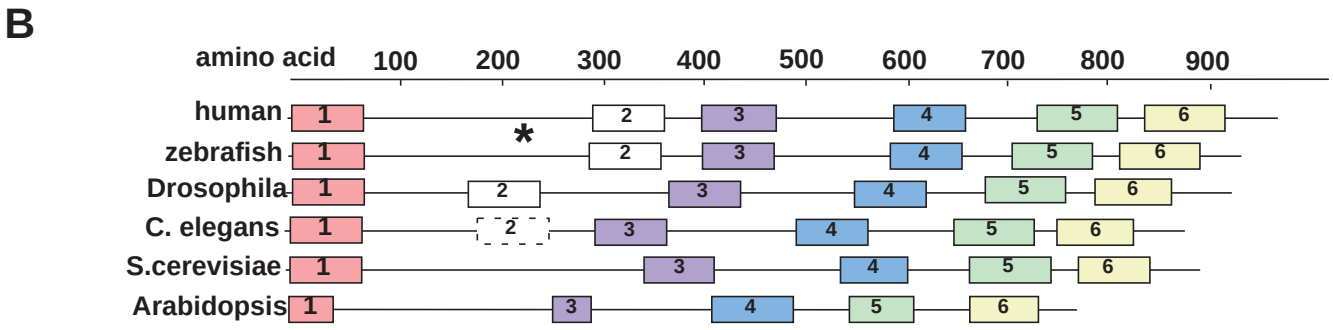

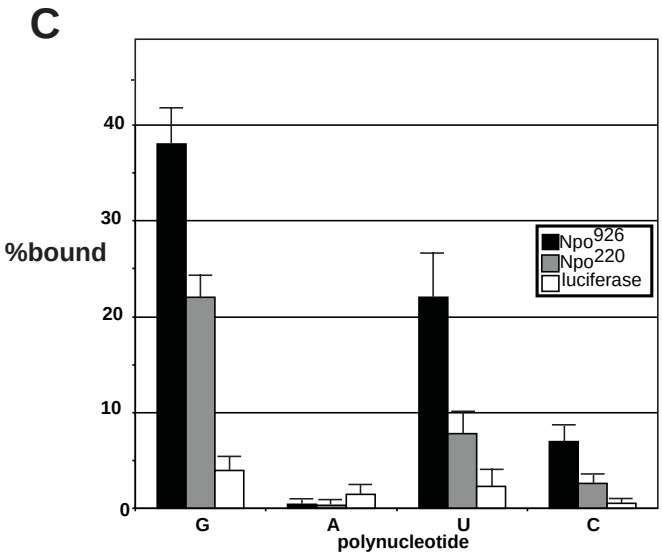

Fig. 6. *npo* encodes a conserved, eukaryotic RNA-binding protein. (A) CLUSTALW alignment of Npo-related proteins from divergent eukaryotes reveals a high degree of conservation, particularly within RRM regions. Dark shading indicates amino acid identity and light shading indicates similarity. Red line indicates canonical RNA recognition motifs. (B) Conservation of RRM-domain configuration between Npo-related proteins. We show a manual alignment of RRM domains identified by RPS blast search of the GenBank conserved domain database (CDD). Domain numbering system was guided by CLUSTALW alignments as shown in panel A. Asterisk indicates site of termination codon encoded by $npo^{fW07\text{-}g}$. GenBank Accession Numbers are as follows: Human, NP_055667; *Drosophila*, AAM29657; *C. elegans*, NP502432; *S. cerevisiae*, NP_015437; *Arabidopsis*, CAB40378. (C) Npo binding of homopolymeric RNA. [^{35}S]-labeled Npo protein produced by in vitro transcription/translation was incubated with solid support-bound homopolymeric RNA of the indicated base composition. After several washes, the radioactivity from bound and input protein was quantitated by autoradiography and digital densitometry. The percent bound was highest for poly G and poly U. Npo^{926} indicates full-length wild-type protein, Npo^{220} indicates the truncated mutant. Error bars indicate±s.e.m. from three independent measurements.

mutant host (Fig. 8D). Out of the 11 single wild-type cells incorporated into the mutant gut epithelium, eight were found to express *ifabp*, indicating that enterocyte-specific transcription had been activated in these cells. Wild-type mesenchymal cells did not appear to rescue subjacent mutant epithelium (0/28). The converse experiment, transplanting mutant cells into wild-type host could not be scored because of a lack of mosaic generation, suggesting a selection against mutant epithelial cells in the wild-type host. These data, taken together with the expression pattern, are consistent with a cell-autonomous requirement for *npo* during gut development.

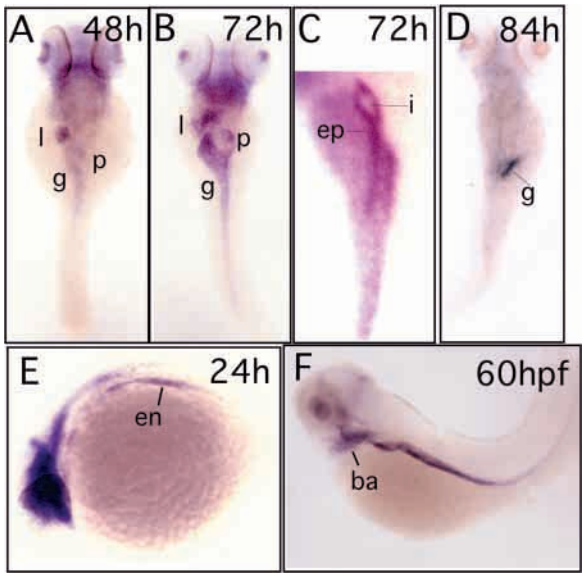

DISCUSSION

We report the identification of the *npo* gene as an essential mediator of intestinal organogenesis in the zebrafish. Early endoderm development and budding of organ primordia proceed independently of the presence of *npo*, but there is arrest at the stage of cytodifferentiation and growth. The

Fig. 7. Developmental expression pattern of *npo*. (A-F) Whole-mount in situ hybridization to *npo* at the indicated developmental stages. (A,B,D) Dorsal view demonstrates dynamic expression in the digestive organ primordia. Expression begins at about 48 hpf, peaks at 72 hpf, then recedes in an anterior to posterior wave around 84 hpf. (C) Right oblique view showing expression of *npo* in the exocrine pancreas at 72 hpf, but not in the pancreatic islet. (E,F) Lateral view showing brain and endoderm expression at 24 hpf, then branchial arch and endoderm expression at 60 hpf. l, liver; g, gut; p, pancreas; i, islet; ep, exocrine pancreas; en, endoderm; ba, branchial arches.

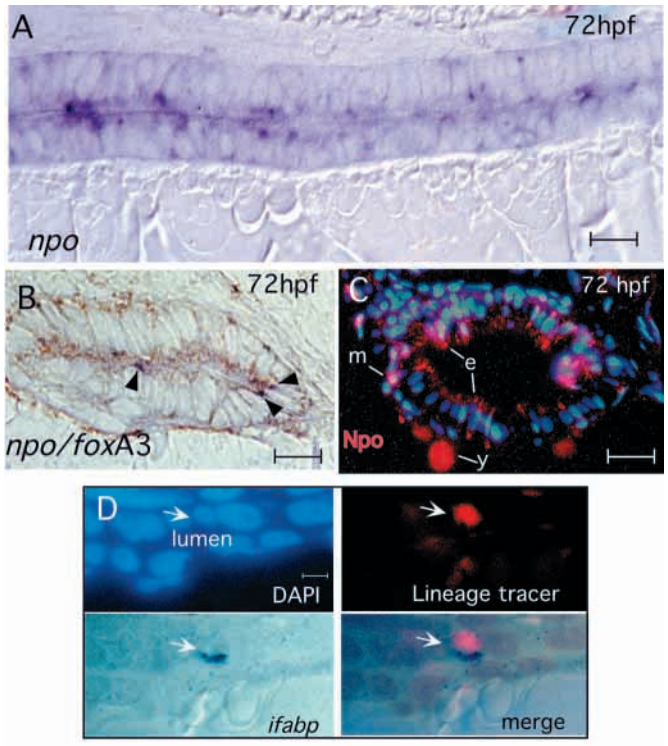

Fig. 8. Expression and function of *npo* in the endoderm. (A) Mid-sagittal section of 72 hpf embryo labeled for *npo* by in situ hybridization, showing punctate, heterogeneous staining in epithelial cells. (B) Double in situ hybridization to *npo* (dark blue; arrowheads) and *foxa3* (brown), showing *npo* expression in a subset of endoderm-derived epithelial cells. (C) Anti-Npo immunofluorescence (red) at 72 hpf shows expression primarily in gut epithelium, and also in scattered subepithelial mesenchymal cells. The yolk signal is caused by autofluorescence. (D) Mosaic analysis: wild-type cell (arrow) in $npo^{-/-}$ host shows cell autonomous rescue of *ifabp* expression. Panels show nuclei (DAPI; blue), lineage tracer (rhodamine dextran; red) and labeling for *ifabp* (dark blue). e, epithelium; m, mesenchyme; y, yolk. Scale bars: A,B, 10 μm; C, 15 μm; D, 7 μm.

freezing of maturation at this particular juncture indicates that the endoderm-intestine transition is subject to unitary genetic control, and *npo* appears to be one crucial element of this switch. *npo* encodes a conserved RRM protein, which suggests that organogenesis may be controlled in part by modulating the activity of putative target RNAs.

The requirement for *npo* reveals a control point during organogenesis

There are many component steps in the formation of the digestive organs, including endoderm formation, primitive gut tube patterning, organ primordium formation, organ cytodifferentiation and organotypic growth (Grapin-Botton and Melton, 2000; Montgomery et al., 1999). The formation of the endoderm depends on the Gata, forkhead and Sox transcription factors (Kikuchi et al., 2001; Reiter et al., 2001), as well as mediators and targets of the TGFβ and WNT signaling pathways (Feldman et al., 2000). Germline mutation of these genes typically leads to early embryonic lethality, precluding the assessment of their function at later stages. As the *npo* mutation does not significantly perturb early endoderm development, and endodermal markers are expressed normally in the mutant, *npo* probably functions subsequent to activity of the endodermal and early organ patterning genes.

After the specification and budding of the anlage, the intestine normally grows and differentiates (Roberts, 1999). This phase is marked by a concerted cell differentiation and rearrangement of the epithelia. Organ-specific programs are then activated to form basic functional units, such as villi or pancreatic acini. Very little is known about the molecular control of the individual processes, or whether their concerted activation reflects a unitary step. In fact, evidence suggests that the patterns of growth unique to each region arise from previous specification events and permissive external cues from the local surrounding mesenchymal tissues (Roberts, 1999). In the *npo*-mutant intestine, the histological appearance of the epithelia remains that of the organ primordium, apical-basal cell polarity is not well established and villi do not form. To our knowledge, there are no genetic mutations in vertebrates displaying this combined phenotype, with both arrested growth and differentiation. For example, the mutation in mice of TCF4 disrupts epithelial stem cell renewal, yet TCF4 is not required for initial villus morphogenesis (Korinek et al., 1998). Disruption of genes required for mesenchymal function, such as *forkhead*6 (Kaestner et al., 1997) and *Pdgfa* (Karlsson et al., 2000), lead to derangement of villus achitecture, but enterocyte differentiation still occurs. The timing of the *npo* phenotype thus implicates the essential role of *npo* in initiating organ-specific morphogenetic and cytodifferentiation programs.

npo expression in the gastrointestinal tract is dynamic, foreshadowing the anterior to posterior wave of rapid organ growth and cytodifferentiation. Overexpression of *npo* causes formation of hyperplastic intestinal and pancreatic epithelium. This result complements the hypoplastic organs seen when *npo* activity is reduced, either by 'knockdown' or germline mutation. Taken together, these data suggest that organ growth and maturation is controlled by *npo* expression in a dose-dependent manner. One possible mechanism by which this could occur is by controlling a specification step common to endoderm-derived epithelia. According to this model, *npo* would promote the adoption of a progenitor phenotype among a subset of organ anlage cells. These cells would then possess the capacity to respond to organ-specific signals that direct their morphogenetic movements and differentiation programs. Perhaps the cell-to-cell variability of *npo* expression in the developing gut (Fig. 8A) reflects the possibility that only a subset of cells are capacitated to form the mature organ. Npo overexpression could thus lead to organ hyperplasia by increasing the number of organ progenitors responding to local signals. In the absence of *npo* function, progenitor cell capacitation would be blocked, leaving the incipient organ arrested as a primordium. That *npo* is needed to specify a gut progenitor cell type is also suggested by its expression in the crpyts of Lieberkuhn of adult mouse intestine (A.N.M. and R. Palmer, unpublished).

Npo is an RRM protein

The *npo* gene encodes a conserved, 926-amino acid protein with six RRM domains. The mutant allele encodes a truncated protein containing only the N-terminal domain, indicating that the remainder of the molecule is necessary for its function in

organogenesis. Immunoreactive Npo is localized to the cell cytoplasm. Although we do not yet know a specific RNA target, it binds RNA with base sequence preference, as do other RRM proteins (Varani and Nagai, 1998).

The role of the Npo protein is not known in metazoans. In yeast, the *npo* ortholog Mrd1p was recently shown to be involved in pre-ribosomal RNA processing (Jin et al., 2002). Mrd1p is detected in complexes containing other proteins known to participate in RNA processing (Gavin et al., 2002). RNA binding proteins have been implicated in numerous developmental processes governed at the RNA level (Curtis et al., 1995). For example, RNA binding may offer a means to rapidly coordinate expression of a diverse subset of target genes that may be functionally related (Keene, 2001; Keene and Tenenbaum, 2002). Accordingly, *npo* might regulate and coordinate the activity of target RNAs important for digestive organ development and homeostasis. For example, some gene products required for epithelial morphogenesis or organ homeostasis are known to occur in multiple splice isoforms. Examples include fibronectin (Huerta et al., 2001; Inoue et al., 2001), epimorphin (Hirai, 2001; Lehnert et al., 2001) and TCF4 (Cho and Dressler, 1998; Young et al., 2002). Given that the Npo-related protein in yeast functions in splicing, it is plausible that, in metazoans, Npo could function by modulating isoform expression of developmentally important targets.

We wish to thank Jau-Nian Chen and the 'Screen Team' for mutagenized zebrafish. We thank Amy Ronco and Mary Mckee for invaluable technical assistance. We are grateful to Daniel Haber and Dan Podolsky for insightful comments and advice. We thank S. Tsukita for anti-ATPase antibody, and P. Ingham and R. Dorsky for probes. Supported by NIH grants 5-R01DK55383-03, 5R01HL63206-02 and 2R01HL49579-08, and a sponsored research agreement with Genentech (M.C.F.); and a Howard Hughes Postdoctoral Fellowship for Physicians and NIH grant K08DK02968 (A.N.M.). The microscopy core facility used in this work was partially supported by a center grant for the study of inflammatory bowel disease (DK43351) and a Boston Area Diabetes Endocrinology Research Center grant (DK57521).

REFERENCES

Allende, M. L., Amsterdam, A., Becker, T., Kawakami, K., Gaiano, N. and Hopkins, N. (1996). Insertional mutagenesis in zebrafish identifies two novel genes, pescadillo and dead eye, essential for embryonic development. *Genes Dev.* **10**, 3141-3155.

Amemiya, C. T., Zhong, T. P., Silverman, G. A., Fishman, M. C. and Zon, L. I. (1999). Zebrafish YAC, BAC, and PAC genomic libraries. *Methods Cell Biol.* **60**, 235-258.

Andre, M., Ando, S., Ballagny, C., Durliat, M., Poupard, G., Briancon, C. and Babin, P. J. (2000). Intestinal fatty acid binding protein gene expression reveals the cephalocaudal patterning during zebrafish gut morphogenesis. *Int. J. Dev. Biol.* **44**, 249-252.

Chantry, A. and Glynn, P. (1986). Two-dimensional electrophoretic characterization of microheterogeneous myelin basic protein fragments. *Anal. Biochem.* **159**, 29-34.

Chen, J. N., van Eeden, F. J., Warren, K. S., Chin, A., Nusslein-Volhard, C., Haffter, P. and Fishman, M. C. (1997). Left-right pattern of cardiac BMP4 may drive asymmetry of the heart in zebrafish. *Development* **124**, 4373-4382.

Chen, J.-N., van Bebber, F., Goldstein, A. M., Serluca, F. C., Jackson, D., Childs, S., Serbedzija, G., Warren, K. S., Mably, J. D., Lindahl, P. et al. (2001). Genetic steps to organ laterality in zebrafish. *Comp. Funct. Genomics* **2**, 60-68.

Cho, E. A. and Dressler, G. R. (1998). TCF-4 binds beta-catenin and is expressed in distinct regions of the embryonic brain and limbs. *Mech. Dev.* **77**, 9-18.

Curtis, D., Lehmann, R. and Zamore, P. D. (1995). Translational regulation in development. *Cell* **81**, 171-178.

Dorsky, R. I., Snyder, A., Cretekos, C. J., Grunwald, D. J., Geisler, R., Haffter, P., Moon, R. T. and Raible, D. W. (1999). Maternal and embryonic expression of zebrafish lef1. *Mech. Dev.* **86**, 147-150.

Edlund, H. (1999). Pancreas: how to get there from the gut? *Curr. Opin. Cell Biol.* **11**, 663-668.

Feldman, B., Dougan, S. T., Schier, A. F. and Talbot, W. S. (2000). Nodal-related signals establish mesendodermal fate and trunk neural identity in zebrafish. *Curr. Biol.* **10**, 531-534.

Gavin, A. C., Bosche, M., Krause, R., Grandi, P., Marzioch, M., Bauer, A., Schultz, J., Rick, J. M., Michon, A. M., Cruciat, C. M. et al. (2002). Functional organization of the yeast proteome by systematic analysis of protein complexes. *Nature* **415**, 141-147.

Grapin-Botton, A. and Melton, D. A. (2000). Endoderm development: from patterning to organogenesis. *Trends Genet.* **16**, 124-130.

Haffter, P., Granato, M., Brand, M., Mullins, M. C., Hammerschmidt, M., Kane, D. A., Odenthal, J., van Eeden, F. J., Jiang, Y. J., Heisenberg, C. P. et al. (1996). The identification of genes with unique and essential functions in the development of the zebrafish, Danio rerio. *Development* **123**, 1-36.

Hirai, Y. (2001). Epimorphin as a morphogen: does a protein for intracellular vesicular targeting act as an extracellular signaling molecule? *Cell Biol. Int.* **25**, 193-195.

Horne-Badovinac, S., Lin, D., Waldron, S., Schwarz, M., Mbamalu, G., Pawson, T., Jan, Y., Stainier, D. Y. and Abdelilah-Seyfried, S. (2001). Positional cloning of heart and soul reveals multiple roles for PKClambda in zebrafish organogenesis. *Curr. Biol.* **11**, 1492-1502.

Huerta, S., Srivatsan, E. S., Venkatesan, N., Peters, J., Moatamed, F., Renner, S. and Livingston, E. H. (2001). Alternative mRNA splicing in colon cancer causes loss of expression of neural cell adhesion molecule. *Surgery* **130**, 834-843.

Inoue, T., Nabeshima, K., Shimao, Y., Meng, J. Y. and Koono, M. (2001). Regulation of fibronectin expression and splicing in migrating epithelial cells: migrating MDCK cells produce a lesser amount of, but more active, fibronectin. *Biochem. Biophys. Res. Commun.* **280**, 1262-1268.

Jin, S. B., Zhao, J., Bjork, P., Schmekel, K., Ljungdahl, P. O. and Wieslander, L. (2002). Mrd1p is required for processing of pre-rRNA and for maintenance of steady-state levels of 40 S ribosomal subunits in yeast. *J. Biol. Chem.* **277**, 18431-18439.

Jowett, T. (1999). Analysis of protein and gene expression. *Methods Cell Biol.* **59**, 63-84.

Kaestner, K. H., Silberg, D. G., Traber, P. G. and Schutz, G. (1997). The mesenchymal winged helix transcription factor Fkh6 is required for the control of gastrointestinal proliferation and differentiation. *Genes Dev.* **11**, 1583-1595.

Karlsson, L., Lindahl, P., Heath, J. K. and Betsholtz, C. (2000). Abnormal gastrointestinal development in PDGF-A and PDGFR-(alpha) deficient mice implicates a novel mesenchymal structure with putative instructive properties in villus morphogenesis. *Development* **127**, 3457-3466.

Katz, J. P., Perreault, N., Goldstein, B. G., Lee, C. S., Labosky, P. A., Yang, V. W. and Kaestner, K. H. (2002). The zinc-finger transcription factor Klf4 is required for terminal differentiation of goblet cells in the colon. *Development* **129**, 2619-2628.

Keene, J. D. (2001). Ribonucleoprotein infrastructure regulating the flow of genetic information between the genome and the proteome. *Proc. Natl. Acad. Sci. USA* **98**, 7018-7024.

Keene, J. D. and Tenenbaum, S. A. (2002). Eukaryotic mRNPs may represent posttranscriptional operons. *Mol. Cell* **9**, 1161-1167.

Kikuchi, Y., Agathon, A., Alexander, J., Thisse, C., Waldron, S., Yelon, D., Thisse, B. and Stainier, D. Y. (2001). casanova encodes a novel Sox-related protein necessary and sufficient for early endoderm formation in zebrafish. *Genes Dev.* **15**, 1493-1505.

Kim, S. K. and Hebrok, M. (2001). Intercellular signals regulating pancreas development and function. *Genes Dev.* **15**, 111-127.

Kimmel, C. B., Ballard, W. W., Kimmel, S. R., Ullmann, B. and Schilling, T. F. (1995). Stages of embryonic development of the zebrafish. *Dev. Dyn.* **203**, 253-310.

Korinek, V., Barker, N., Moerer, P., van Donselaar, E., Huls, G., Peters, P. J. and Clevers, H. (1998). Depletion of epithelial stem-cell compartments in the small intestine of mice lacking Tcf-4. *Nat. Genet.* **19**, 379-383.

Lehnert, L., Lerch, M. M., Hirai, Y., Kruse, M. L., Schmiegel, W. and Kalthoff, H. (2001). Autocrine stimulation of human pancreatic duct-like development by soluble isoforms of epimorphin in vitro. *J. Cell Biol.* **152**, 911-922.

Lewis, K. E., Concordet, J. P. and Ingham, P. W. (1999). Characterisation of a second patched gene in the zebrafish Danio rerio and the differential response of patched genes to Hedgehog signalling. *Dev. Biol.* **208**, 14-29.

Milewski, W. M., Duguay, S. J., Chan, S. J. and Steiner, D. F. (1998). Conservation of PDX-1 structure, function, and expression in zebrafish. *Endocrinology* **139**, 1440-1449.

Montgomery, R. K., Mulberg, A. E. and Grand, R. J. (1999). Development of the human gastrointestinal tract: twenty years of progress. *Gastroenterology* **116**, 702-731.

Odenthal, J. and Nusslein-Volhard, C. (1998). fork head domain genes in zebrafish. *Dev. Genes Evol.* **208**, 245-258.

Pack, M., Solnica-Krezel, L., Malicki, J., Neuhauss, S. C. F., Schier, A. F., Stemple, D. L., Driever, W. and Fishman, M. C. (1996). Mutations affecting development of zebrafish digestive organs. *Development* **123**, 321-328.

Reiter, J. F., Kikuchi, Y. and Stainier, D. Y. (2001). Multiple roles for Gata5 in zebrafish endoderm formation. *Development* **128**, 125-135.

Roberts, D. (1999). Embryology of the Gastrointestinal Tract. In *Development of the Gastrointestinal Tract* (ed. I. A. Sanderson and W. A. Walker), pp. 1-12. Hamilton: B. C. Decker.

Schilling, T. F., Piotrowski, T., Grandel, H., Brand, M., Heisenberg, C. P., Jiang, Y. J., Beuchle, D., Hammerschmidt, M., Kane, D. A., Mullins, M. C. et al. (1996). Jaw and branchial arch mutants in zebrafish I: branchial arches. *Development* **123**, 329-344.

Shimoda, N., Knapik, E. W., Ziniti, J., Sim, C., Yamada, E., Kaplan, S., Jackson, D., de Sauvage, F., Jacob, H. and Fishman, M. C. (1999). Zebrafish genetic map with 2000 microsatellite markers. *Genomics* **58**, 219-232.

Swanson, M. S. and Dreyfuss, G. (1988). Classification and purification of proteins of heterogeneous nuclear ribonucleoprotein particles by RNA-binding specificities. *Mol. Cell. Biol.* **8**, 2237-2241.

Traber, P. G. and Wu, G. D. (1995). Intestinal Development and Differentiation. In *Gastrointestinal Cancers: Biology, Diagnosis and Therapy* (ed. A. K. Rustgi), pp. 21-43. Philadelphia: Lippincott-Raven.

Varani, G. and Nagai, K. (1998). RNA recognition by RNP proteins during RNA processing. *Annu. Rev. Biophys. Biomol. Struct.* **27**, 407-445.

Wessells, N. K. and Cohen, J. H. (1967). Early pancreas organogenesis: morphogenesis, tissue interactions, and mass effects. *Dev. Biol.* **15**, 237-270.

Westerfield, M. (1995). *The Zebrafish Book*. Eugene: The University of Oregon Press.

Yang, Q., Bermingham, N. A., Finegold, M. J. and Zoghbi, H. Y. (2001). Requirement of Math1 for secretory cell lineage commitment in the mouse intestine. *Science* **294**, 2155-2158.

Young, R. M., Reyes, A. E. and Allende, M. L. (2002). Expression and splice variant analysis of the zebrafish tcf4 transcription factor. *Mech. Dev.* **117**, 269-273.

Zaret, K. S. (2000). Liver specification and early morphogenesis. *Mech. Dev.* **92**, 83-88.